Energy Proceedings
Vol 28, 2022
ISSN 2004-2965

Numerical study on the performance of a dew-point evaporative cooler with a desiccant coated heat exchanger

Seung Jin Oh[1,*], Yeongmin Kim[1], Byng Chan Kang[2], Yong-yoo Yang[1], Yoon Jung Ko[1], Eun I Kim[1], Kim Choon Ng[3]

[1] *Sustainable Technology and Wellness R&D group, Korea Institute of Industrial Technology, Jeju-si, Jeju special Self-Governing Province, Korea*

[2] *Local Energy R&D Center, Jeju Energy Corporation, Jeju-si, Jeju special Self-Governing Province, Korea*

[3] *Water Desalination and Reuse Center, BESE Div., King Abdullah University of Science and Technology, Thuwal, Saudi Arabia,*

ABSTRACT

This study presents an innovative de-coupling cooling technology where latent cooling load and sensible cooling load are handled separately by a desiccant coated heat exchanger (DCHE) based dehumidifier and a dew-point evaporative cooler (DEC). Their performances are investigated numerically by analyzing the heat and mass transfer. Simulation has been carried out for DCHE and examined the output states of the process air, namely the dry-bulb temperature and humidity ratio. Key results revealed that moisture removal capacity (MRC), latent cooling capacity (Q_L) for DCHE are largely affected by varying air dry-bulb and air wet-bulb temperatures while the almost constant COP_{th} was observed regardless of the variation of temperatures. For the DEC, the higher dew-point effectiveness and wet-bulb effectiveness were observed at the higher dry-bulb temperature and higher humidity ratio while the higher sensible cooling capacity was observed at the higher dry-bulb temperature and lower humidity ratio.

Keywords: de-coupling cooling system, desiccant coated heat exchanger, dew-point evaporative cooler, moisture removal capacity, dew-point effectiveness

1. INTRODUCTION

The growing population and rising energy demand in many countries are imposing significant challenges to energy and environmental sustainability. The global energy and environmental scenarios are closely interlinked. That is, the problems of supply and use of energy are related to global warming and climate change[1]. The electrical energy consumption for air conditioning accounts for 20-40% of the total electricity used in buildings around the world today[2,3]. Global energy demand for air conditioning is expected to triple by 2050, requiring new electricity capacity that is the equivalent to the combined electricity capacity of the United States, the EU and Japan today. Accordingly, the global stock of air conditioners in buildings will grow to 5.6 billion by 2050, up from 1.6 billion today, which means new air conditioners is sold every second for the next 30 years[4].

In conventional air-conditioning systems, the compressor efficiency has leveled asymptotically, implying that efficiency improvement for compressor stages and heat exchangers have been saturated. There are physical and material limits to which efficiency improvement of the major components in the cooling cycle can be attained. Therefore, we believe that there is a need for an out-of-box solution for cooling where the consumption of energy and water can be reduced significantly, by as much as 50% so as to attain sustainable cooling for the future, addressing the space cooling needs of the present and future generations.

In this study, firstly, we present an innovative de-coupling cooling technology where latent cooling load and sensible cooling load are handled separately by a desiccant coated heat exchanger (DCHE) based dehumidifier and a dew-point evaporative cooler (DEC). Secondly, the performance is investigated numerically by analyzing the heat and mass transfer for both DCHE and the DEC.

2. WORKING PRINCIPLE

Figure 1 shows schematically the working principle of the de-coupling system and its thermodynamic process on a psychrometric chart. The DCHE first removes the undesired moisture of humid outdoor air by the adsorption process. Subsequently, the DEC cools down the dehumidified air up to the desired temperature, maintaining moisture level. It is noteworthy that the proposed system can handle all climate conditions successfully as well as it employs only waste heat for the regeneration of adsorbent, and the IEC uses only water as a refrigerant.

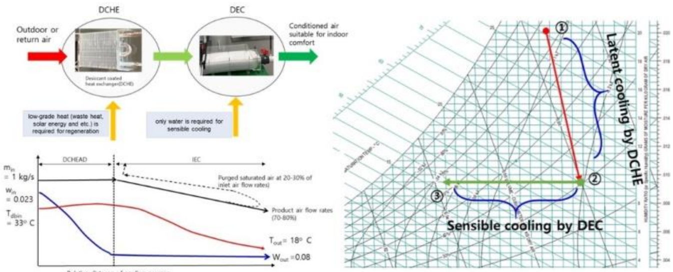

Fig. 1 The working principle of the de-coupling cooling system

2.1 Desiccant coated heat exchanger-based dehumidification (DCHE)

The desiccant coated heat exchanger (DCHE) has been tested successfully for dehumidification application using only the low temperature waste heat, as proven in the many case studies[2,5–7]. It could remove effectively moisture from humid air at a relative humidity ratio of 95% or a humidity ratio of above 20 g/kg using commercial adsorbents such as the silica gel, Zeolite and MOF.

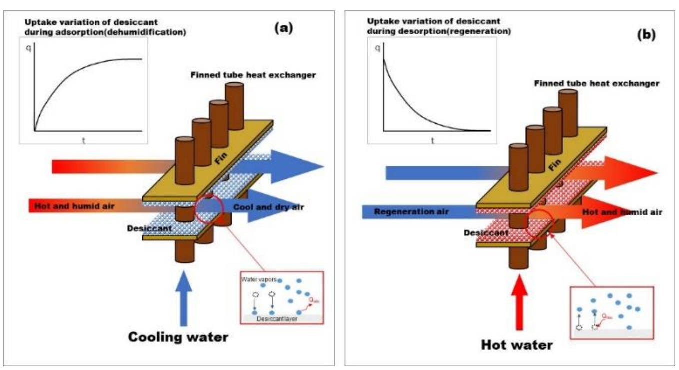

Fig. 2 The concept of the desiccant coated heat exchanger (DCHE) for the dehumidification: (a) adsorption/dehumidification process (b) desorption/regeneration process

The optimal coating thickness of the desiccant layer is found to be 0.1 mm in many studies[8–10]. As depicted in figure 2, the DCHE operates alternatively between two different modes, namely dehumidification (adsorption) mode, and regeneration (desorption) mode. During the dehumidification mode, cooling water is supplied through the tubes in order to remove the adsorption heat, keeping the desiccant layer at a lower temperature and thus ensuring the highest uptake. On the other hand, hot water is supplied to release the water vapor that was adsorbed in the previous process during the regeneration mode. In this mode, each process continues until the uptake reaches the equilibrium uptake given the temperature and vapor pressure.

2.2 Dew-point evaporative cooler (DEC)

As one of evaporative cooling methods, the dew-point evaporative cooler (DEC) is an energy-efficient and environmentally-friendly sensible cooling device that employs only water as a refrigerant[11–13]. The working principles for three different evaporative coolers are represented in figure 3.

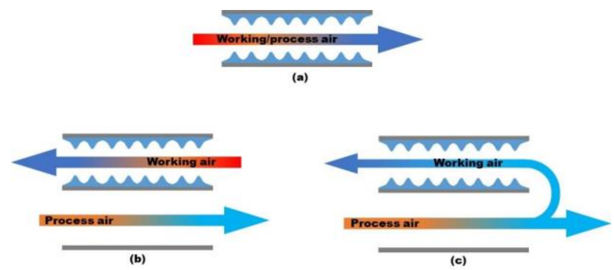

Fig. 3 The working principles of evaporative cooling devices: (a) direct evaporative cooler (b) indirect evaporative cooler (c) dew-point evaporative cooler

The DEC differs from the conventional adiabatic cooling or commonly known as the cooling towers, swarm coolers, etc., where the air stream experience changes in both the temperature and absolute humidity. In the DEC, however, the product air (conditioned air for space cooling) is flowing in a dry channel whilst a small fraction (20 to 30%) of the product air is purged into a wet channel, where the purged air picks up the water vapor from a hydrophilic membrane that physically separates the evaporative moist air flowing in a counter-flow direction from the product air. The evaporative cooling in the wet channel cools the air flowing in the adjacent dry channel by heat transfer and the processes are repeated in succession to achieve an overall cooling of primary air. At the end of a section, the saturated secondary air is purged whilst a part of the conditioned primary air (but at the original inlet humidity) is directed into the wet channel to repeat the evaporative cooling. Thermodynamically, it incurs two major energy losses to achieve cooling of the primary air stream: Firstly, energy is transferred to the air by a fan for maintaining the necessary air flows in all channels. Secondly, it continuously purges a fraction of the conditioned air of the non-wetted channel so as to re-initiate the evaporative cooling in successive wetted-channels. The key feature here is that it continuously purges a fraction of the conditioned air so that the wet-bulb temperature of the conditioned stream can be lowered. The novelty of the de-coupling cycle is the harnessing of evaporative potential of inlet air as well as waste heat but the overall electricity incurred is a quantum lower than that of conventional chillers.

3. MATHEMATICAL MODELLING

3.1 DCHE

In order to investigate the heat and mass transfer for the DEC, a mathematical model was established. The differential control volume includes half the height of the dry and wet channels, the separating plate, and the water film. To simplify the heat and mass transfer processes, the following assumptions were made:

Mass transfer between the adsorbent (desiccant) and adsorbate (water vapor) can be expressed by LDF (Linear Driving force) model as following:

$$\frac{dq}{dt} = k(q^* - q) \tag{1}$$

where dq/dt is the rate of the uptake of water vapor, q* is the equilibrium uptake. k is a reaction coefficient and can be obtained by

$$k = \frac{15D_{so}exp\left(-\frac{E_a}{RT_d}\right)}{R_p^2} \tag{2}$$

where D_{so} a diffusion coefficient and E_a is an activation energy, R is a universal gas constant, Td is the desiccant temperature, R_p is an average radius of desiccant particles respectively. These values are listed in Table 2. The equilibrium uptake, q*, can be approximated with Tóth model.

$$\frac{q^*}{q_0} = \frac{K_T P exp\left(\frac{Q_{st}}{RT}\right)}{\left\{1+\left[K_T exp\left(\frac{Q_{st}}{RT}\right)\right]^t\right\}^{1/t}} \tag{3}$$

where q_0 is the maximum uptake of the desiccant and can be obtained by the measured isotherm. Q_{st} is the isosteric heat of the desiccant, t is heterogeneity factor, K_T is Tóth constant, P is the vapor partial pressure.

The energy conservation equation of DCHE during adsorption/desorption process can be expressed by the following equation:

$$\left[M_d c_{p,d} + M_{hx} c_{p,hx} + M_d c_{p,v} q(t)\right] \frac{dT_d}{dt} = M_d \frac{dq}{dt} Q_{st} - \dot{m}_a c_{p,a}\left(T_{a,o} - T_{a,i}\right) - \dot{m}_w c_{p,w}\left(T_{w,o} - T_{w,i}\right) \tag{4}$$

Mass conservation equation of adsorbed phase of water vapor in the desiccant can be expressed by the following equation:

$$M_d \frac{dq}{dt} = \dot{m}_{v,in} - \dot{m}_{v,out} \tag{5}$$

$\dot{m}_{v,in}$ and $\dot{m}_{v,out}$ are the mass flow rate of the moisture in the air at the inlet and outlet of DCHE respectively. The humidity ratio of the air at the outlet can be calculated by equation (6).

$$\omega_o = \frac{\dot{m}_{v,o}}{\dot{m}_{da}} \tag{6}$$

where $\dot{m}_{da}$ is the mass flow rate of dry air. It should be noted that the mass flow rate of dry air remains constant during the dehumidification and regeneration processes.

The temperature of the process air at the outlet of DCHE is obtained by the following equation:

$$T_{a,o} = \left(T_d - T_{a,i}\right) exp\left(-\frac{A_{c,a} h_{c,a}}{\dot{m}_a c_{p,a}}\right) \tag{7}$$

$$T_{w,o} = \left(T_d - T_{w,i}\right) exp\left(-\frac{A_{c,w} h_{c,w}}{\dot{m}_w c_{p,w}}\right) \tag{8}$$

3.2 DEC

The mathematical model was for a differential control volume including half the height of the dry and wet channels, the separating plate, and the water film.

In the dry channel of DEC, only a sensible cooling effect takes place by forced convective heat transfer without changing the humidity ratio. The energy conservation equation for air flowing in the dry channel is expressed by

$$k_a \frac{d^2 T_{da}}{dx^2} - u_{da} \rho_{da} c_{p,m} \frac{\partial T_{da}}{dx} = \frac{h_{da}}{\bar{H}} \left(T_{da} - T_p\right) \tag{9}$$

Unlike the dry channel, both sensible and latent cooling effects take place in the wet channel. That is, both heat and mass transfer mechanism are involved to create cooling effect between the air and water film layer, and it is expressed as follows:

$$k_a \frac{d^2T_{wa}}{dx^2} + u_{da}\rho_{da}c_{p,m}\frac{dT_{wa}}{dx} = \frac{h_{wa}}{\bar{H}}(T_{wa} - T_f) + \frac{h_m\rho_{da}}{\bar{H}}[\omega_{sat}(T_f) - \omega_v]c_{p,v}(T_{wa} - T_f) \quad (10)$$

The mass transfer takes place only in the wet channel by the driving force of vapor partial pressure difference, and the mass conservation equation is written as

$$\rho_{da}D_v\frac{d^2\omega_v}{dx^2} = -\rho_{da}u_{wa}\frac{d\omega_v}{dx} + h_m\bar{H}\rho_{da}(\omega_{v,sat}(T_f) - \omega_v) \quad (11)$$

On the other hand, the energy balances for the water film and the separating plate are given as

$$k_f\frac{d^2T_f}{dx^2} = -\frac{h_w(T_{wa}-T_f)}{\delta_f} - k_f\frac{T_p-T_f}{\delta_f^2} + \frac{h_{fg}h_m\rho_{da}[\omega_{sat}(T_f)-\omega]}{\delta_f} \quad (12)$$

$$k_p\frac{d^2T_p}{dx^2} = -\frac{h_d(T_{da}-T_p)}{\delta_p} + \frac{k_p(T_p-T_f)}{\delta_p^2} \quad (13)$$

4. METHODOLOGY

The heat and mass transfer analysis for the de-coupled cooling system has been carried out using the developed mathematical models. Variable order method (ode15s) was employed for the transient simulation of DCHE and fourth order method (bvp4c) for the steady-state simulation of DEC in MATLAB platform. As shown in Table 2, moderate climate conditions (T_{db}=35 °C T_{wb}=24 °C) were considered as the baseline, and the cool climates are adopted for the lower limit condition and hot climates for the upper limit conditions.

Table 2. Simulation conditions for DCHE.

Operation parameters	Baseline	Values
Process air inlet dry-bulb temperature [°C]	35	27, 30, 40, 46
Process air inlet wet-bulb temperature [°C]	24	19, 22, 24, 26
Process/regeneration air mass flow rate [kg/h]	13	
Cooling water inlet temperature [°C]	30	25, 30, 35
Hot water inlet temperature [°C]	80	50, 60, 70, 80
Cycle time [sec.]	150	

The performance of DCHE was examined by analyzing two different metrics namely, moisture removal capacity (MRC) and latent cooling capacity (Q_L), and coefficient of performance (COP_{th}). MRC is defined as the total amount of water vapor that is absorbed by the desiccant during the dehumidification process, and Q_L is defined as the cooling power to remove the moisture. They can be calculated by the equation shown in Table 3.

Table 3. Performance indices.

Index	equation
Moisture removal capacity	$MRC = \int_{t_0}^{t} \dot{dv}\, dt$
Coefficient of performance	$COP_{th} = \frac{Q_l}{\dot{m}_{hw}(T_{hw,in} - T_{hw,out})}$
Cooling power	$Q_l = H_v \times \dot{m}_{da}(\dot{\omega}_{in} - \omega_{out})$
Sensible cooling capacity	$Q_S = (1-\gamma)\dot{m}_{da}(T_{da,in} - T_{da,out})$
wet-bulb effectiveness	$\varepsilon_{wb} = \frac{T_{da,in} - T_{da,out}}{T_{da,in} - T_{wb}(T_{da,in})}$
and dew-point effectiveness	$\varepsilon_{db} = \frac{T_{da,in} - T_{da,out}}{T_{da,in} - T_{db}(T_{da,in})}$

5. RESULTS AND DISCUSSIONS

5.1 Performance of DCHE

The performance of the DCHE was numerically analyzed, and simulation results are judiciously compared through a series of runs under various operating conditions. Figure 4 shows the dynamic variation of the performance of DCHE during 3 cycles under the baseline conditions where. It is easily seen from figure 4 (a) that the equilibrium uptake reaches its saturated state at 0.33 during the dehumidification process, and at 0.12 during the regeneration process at a given condition. It is also seen that the actual uptake follows the trajectory of the equilibrium uptake at a different rate. It can also be observed from figure f (b) that the outlet humidity ratio reaches its equilibrium state at a faster rate during the regeneration process. However, it is noteworthy that the amount of the vapor that is released and adsorbed by the desiccant is conserved during the cycle so that the system continues to operate at a cyclic steady state. The lowest humidity ratio of 0.0092 kg_v/kg_{da} was observed at 16 seconds after the dehumidification process starts and then it increases gradually up to its saturated level.

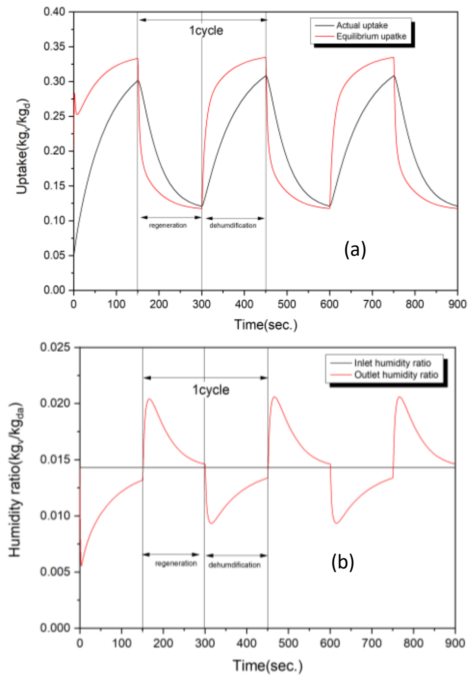

Fig. 4 Dynamic variations of the performance of the DCHE under the baseline conditions :(a) the variations of instantaneous uptake and the equilibrium uptake; (b) The variation of the air humidity ratio at the outlet of DCHE.

Figure 5 shows the effect of change in the dry-bulb temperature of the process air on the performance of DCHE, namely, moisture removal capacity (MRC), COP_{th}, latent cooling capacity (Q_l), and regeneration energy (Q_{reg}). The dry-bulb temperature varied from 27 °C to 46 °C while the other parameters were kept constant as in the baseline conditions. It is observed that MRC, Ql, and Qreg are markedly affected by process air inlet dry-bulb temperature whereas COPth remains constantly around 0.125. MRC drops by 23.6% from 1.867 (T_{db} =35 ^{o}C) to 1.42 (T_{db}=46 ^{o}C). This is mainly because the humidity ratio decreases from 0.0142 to 0.0096, which implies the air carries less water vapor at a higher temperature when wet-bulb temperate is fixed at constant.

Figure 6 shows the effect of change in the wet-bulb temperature of the process air on the performance of DCHE. Unlike the previous results, the performance indices are raised when increasing the wet-bulb temperature except for COP_{th}. The highest values for MRC, Q_l and Q_{reg} were 1.87 g/cycle and 30.1 W respectively when T_{wb}= 24 ^{o}C. It can be observed that MRC, Q_l and Q_{reg} decreases slightly at T_{wb}=26 ^{o}C.

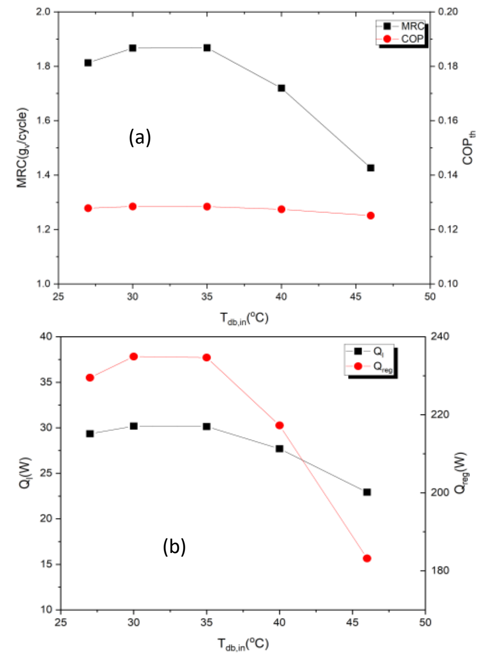

Fig. 5 Effect of change in the process air dry-bulb temperature on the performance of DCHE: (a) moisture removal capacity (MRC) and COP_{th}; (b) latent cooling capacity (Q_l) and regeneration energy (Q_{reg})

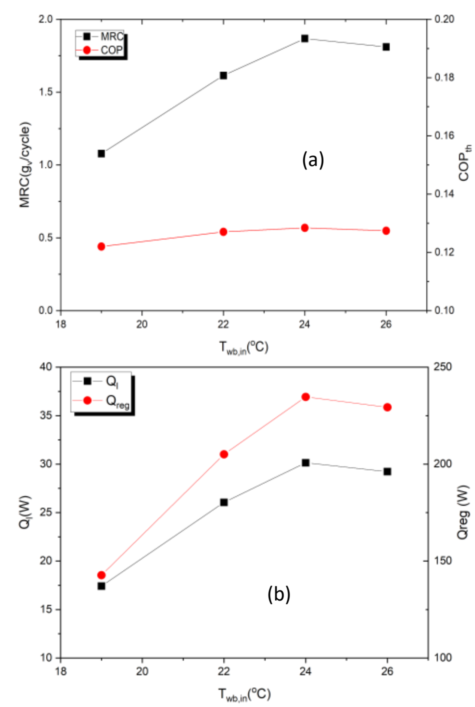

Fig. 6. Effect of change in the process air wet-bulb temperature on the performance of DCHE: (a) moisture removal capacity (MRC) and COP_{th}; (b) latent cooling capacity (Q_l) and regeneration energy (Q_{reg}).

5.2 Performance of DEC

Figure 7 depicts the temperature and humidity ratio profiles of the product air and the working air for DEC under a specified operating condition. The product air flows along the channel length and the working air flow reversely in a counter flow manner. It is observed from figure 9 (b) that the product air is purged at the end of the channel and is flowed back to the inlet. The product air temperature drops sensibly from 26 °C to 16.18 °C while the working air temperature increases from 16.8 °C to 24 °C. It can be found that the temperature drops significantly within a distance of 0.1 m from the end of the channel immediately after being purged. This is because that instantaneous evaporation takes place from the surface of the water film by the continuously purged air. As depicted n Figure 9 (b), the relative humidity surges rapidly from 0.4 to 0.98 in the immediate vicinity of the exit. In addition, once the actual humidity ratio reaches the saturation level, both humidity ratios increases gradually which allows for water to evaporate continuously along the channel length.

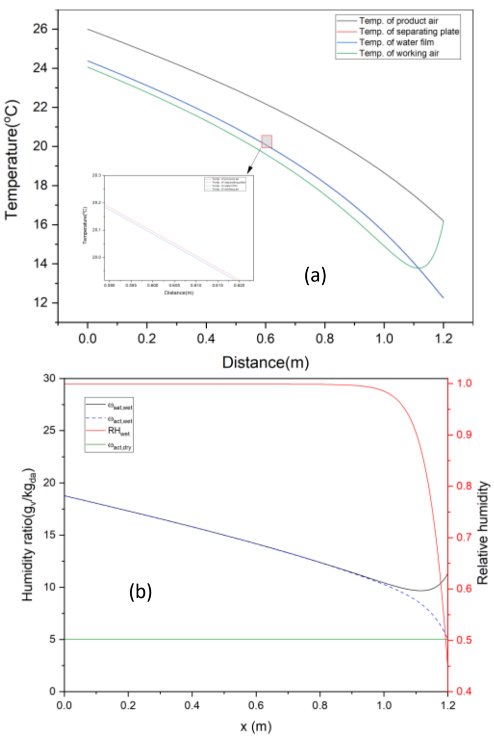

Fig. 7 Temperature profile (a) and humidity ratio profile (b) of each component in DEC.

Figure 8 depicts the effect of change in the air temperature and humidity ratio on the performance of DEC while other parameters are kept constant as in the baseline conditions. The dry-bulb temperature varies from 26 °C to 38 °C, and the humidity ratio varies from 0.005 kg_v/kg_{da} to 0.0187 kg_v/kg_{da} respectively. It can be found that the performance indices are almost linearly dependent on the air dry-bulb temperature and the humidity ratio. For the dew-point effectiveness, it varies between 0.44 and 0.57 when the dry-bulb temperature varies from 26 °C to 38 °C. It can be inferred that the higher the air temperature is the higher the dew-point effectiveness. It should be noted that the higher dew-point effectiveness and the wet-bulb effectiveness can be expected at a higher humidity ratio whereas higher cooling capacity can be obtained at a lower humidity ratio. This is because both wet-bulb and dew-point temperatures increase in proportion to the humidity ratio when the dry-bulb temperature is fixed. Therefore, the potential for water evaporation is declined and thus the temperature drop in the dry channel gets closer to its maximum (i.e. 1).

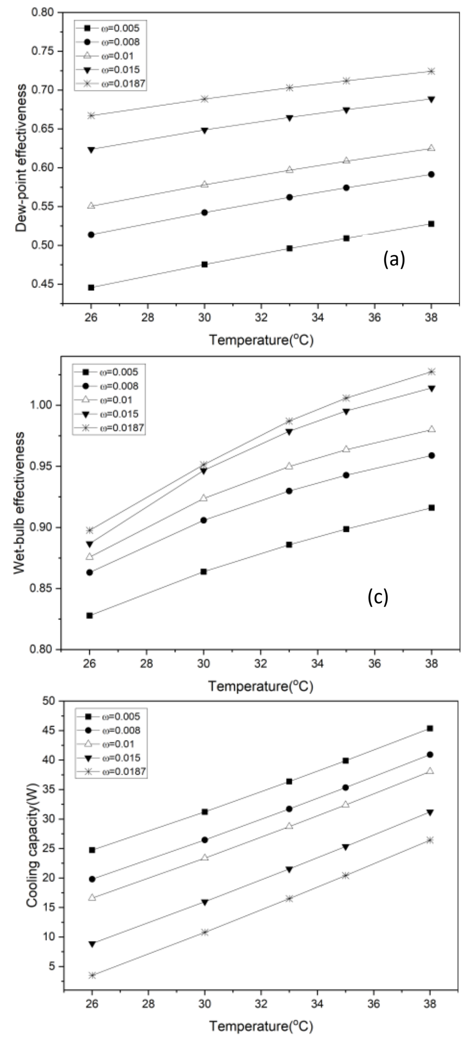

Fig. 8 Effect of change in the air temperature and humidity ratio on the performance of DEC: (a) dew-point effectiveness, (b) wet-bulb effectiveness, and (c) cooling capacity

6. CONCLUSION

This study presents an innovative de-coupling cooling technology where latent cooling load and sensible cooling load are handled separately by a desiccant coated heat exchanger (DCHE) based dehumidifier and a dew-point evaporative cooler (DEC).

The DCHE first removes the undesired moisture of humid outdoor air by adsorption process. Subsequently, the DEC sensibly cools down the dehumidified air up to the desired temperature, maintaining the moisture level. Their performances are investigated numerically by analyzing the heat and mass transfer. Simulation has been carried out for DCHE and examined the output states of the process air, namely the dry-bulb temperature and humidity ratio. The following findings can be inferred from this study:

(1) The equilibrium uptake reaches its saturated state at 0.33 during the dehumidification process, and at 0.12 during the regeneration process at a given condition. The actual uptake follows the trajectory of the equilibrium uptake at a different rate.

(2) MRC and Q_l of the DCHE were markedly affected by varying the dry-bulb temperature and wet-bulb temperature whereas COP_{th} remained constantly around 0.125. The MRC drops by 23.6% at higher temperature was observed due to the decreases in the humidity ratio.

(3) As the wet-bulb temperature of the process air increases, the improved MRC and Q_l of the DCHE were observed due to the increases in the humidity ratio.

(4) For the DEC, dew-point effectiveness, wet-bulb effectiveness and cooling capacity were linearly dependent on the dry-bulb temperature of the process air as well as the humidity ratio.

(5) The higher dew-point effectiveness and the wet-bulb effectiveness can be expected at a higher humidity ratio whereas higher cooling capacity can be obtained at a lower humidity ratio.

The proposed de-coupling system has no moving parts and harmful refrigerant, rendering less maintenance compared to an existing cooling system. Furthermore, it is an energy-efficient means of latent and sensible cooling by adsorption process and water evaporation process with a waste heat source as compared to other conventional air-conditioning processes.

ACKNOWLEDGEMENT

This work was supported by the Renewable Surplus Sector Coupling Technology Program of the Korea Institute of Energy Technology Evaluation and Planning (KETEP) granted financial resource from the Ministry of Trade, Industry & Energy, Republic of Korea (No. 20226210100050)

REFERENCE

[1] Shahzad MW, Burhan M, Ang L, Ng KC. Energy-water-environment nexus underpinning future desalination sustainability. Desalination 2017;413:52–64. https://doi.org/10.1016/j.desal.2017.03.009.

[2] Oh SJ, Ng KC, Chun W, Chua KJE. Evaluation of a dehumidifier with adsorbent coated heat exchangers for tropical climate operations. Energy 2017;137:441–8. https://doi.org/10.1016/j.energy.2017.02.169.

[3] Oh SJ, Ng KC, Thu K, Chun W, Chua KJE. Forecasting long-term electricity demand for cooling of Singapore's buildings incorporating an innovative air-conditioning technology. Energy Build 2016;127:183–93. https://doi.org/10.1016/j.enbuild.2016.05.073.

[4] International Energy Agency, The future of Cooling 2018.

[5] SJ Oh, K Choon Ng, K Thu, M Kum Ja, MR Islam, W Chun KC. Studying the performance of a dehumidifier with adsorbent coated heat exchangers for tropical climate operations.pdf. Sci Technol Built Environ 2017;23:127–35.

[6] Hu LM, Ge TS, Jiang Y, Wang RZ. Performance study on composite desiccant material coated fin-tube heat exchangers. Int J Heat Mass Transf 2015;90:109–20. https://doi.org/10.1016/j.ijheatmasstransfer.2015.06.033.

[7] Ge TS, Dai YJ, Wang RZ, Li Y. Feasible study of a self-cooled solid desiccant cooling system based on desiccant coated heat exchanger. Appl Therm Eng 2013;58:281–90. https://doi.org/10.1016/j.applthermaleng.2013.04.059.

[8] Hyun M, Oh SJ. Numerical Study on Dehumidification Performance of a Desiccant Coated Heat Exchanger n.d.

[9] Oh SJ, Ng KC, Chun W, Chua KJE. Evaluation of a dehumidifier with adsorbent coated heat exchangers for tropical climate operations. Energy 2017;137:441–8. https://doi.org/10.1016/j.energy.2017.02.169.

[10] Tu YD, Wang RZ, Hua LJ, Ge TS, Cao BY. Desiccant-coated water-sorbing heat exchanger: Weakly-coupled heat and mass transfer. Int J Heat Mass Transf 2017;113:22–31. https://doi.org/10.1016/j.ijheatmasstransfer.2017.05.047.

[11] Lin J, Thu K, Bui TD, Wang RZ, Ng KC, Chua KJ. Study on dew point evaporative cooling system with counter-flow configuration. Energy Convers Manag 2016;109:153–65. https://doi.org/10.1016/j.enconman.2015.11.059.

[12] Lin J, Bui DT, Wang R, Chua KJ. On the fundamental heat and mass transfer analysis of the counter-flow dew point evaporative cooler. Appl Energy 2018;217:126–42. https://doi.org/10.1016/j.apenergy.2018.02.120.

[13] Riangvilaikul B, Kumar S. An experimental study of a novel dew point evaporative cooling system. Energy Build 2010;42:637–44. https://doi.org/10.1016/j.enbuild.2009.10.034.